Threshold characteristic of intracavity optical parametric oscillator pumped by all-solid-state Q-switched laser

Yuye Wang (王与烨)[1], Degang Xu (徐德刚)[1], Yizhong Yu (于意仲)[1], Wuqi Wen (温午麒)[1], Xifu Li (李喜福)[2], and Jianquan Yao (姚建铨)[1]

[1]*College of Precision Instrument and Optoelectronics Engineering, Institute of Laser and Optoelectronics, Tianjin University, Tianjin 300072*

Cooperated Institute of Nankai University and Tianjin University, Tianjin 300072

Key Laboratory of Optoelectronic Information Science and Technology, Ministry of Education, Tianjin University, Tianjin 300072

[2]*School of Electrical Engineering and Automation, Tianjin University, Tianjin 300072*

Received August 28, 2007

We derive the threshold pump intensity for a singly resonant intracavity optical parametric oscillator (IOPO) based on a temporal coupled field model. Particular attention is paid to the dependence of the intracavity singly resonant OPO (SRO) threshold intensity on the signal wave output coupling. Meanwhile, a Nd:YAG laser pumped $KTiOPO_4$ (KTP) IOPO for eye-safe laser output is studied experimentally. The experiment is performed with four signal wave output reflectivities of 60%, 70%, 80%, and 90%, respectively. The measured values are in good agreement with the theoretical results. With an output coupler reflectivity of 80%, a peak power of 70 kW at 1572 nm has been obtained at a repetition rate of 3.5 kHz. The pulse width is 4.9 ns. Such investigation is helpful to identifying suitable operational regime of low pump intensity.

OCIS codes: 190.4970, 140.3540, 140.3480.

Eye-safe laser sources have many applications in remote sensing, pollution detection, and laser radar. One of the promising ways to obtain eye-safe wavelength region ($1.5-1.6$ μm) is optical parametric oscillator (OPO).

According to the position of the OPO cavity, there are two different schemes of OPOs: intracavity optical parametric oscillator (IOPO) and extracavity optical parametric oscillator (EOPO). Typically, EOPO consists of a separate pulsed pump laser and an OPO cavity. The threshold of this configuration is very high, which limits the repetition rate of the pump laser (usually hertz magnitude) and cannot meet the needs of some applications such as high-repetition-rate laser radar. Moreover, it stimulates the requirement for powerful pump sources and high-damage-threshold nonlinear crystal. Compared with EOPO, IOPO is to place the OPO cavity inside the cavity of the pump laser. It can take advantage of high fundamental power density within the oscillator to realize a low threshold and high efficiency[1−3]. Thus IOPO is widely applied into high-repetition-rate eye-safe laser[4−7]. From the 1960s to 1990s, the threshold pump intensities for both extracavity singly and doubly resonant parametric oscillators have been extensively studied and developed[8−14]. In the theoretical models of Brosnan-Byer[10] and Guha-Wu-Falk[11], it was assumed that the signal spot sizes were determined directly by the pump spot size and by its optical cavity, respectively. Subsequently, some researchers[15−17] have amended the threshold pump intensity for a singly resonant OPO (SRO) of Brosnan-Byer model. Their calculated thresholds were in reasonable agreement with the measured values in many experiments of EOPOs. However, the threshold pump intensity for IOPO was studied far less than that of EOPO. Although Debuisschert *et al.*[18] and Turnbull *et al.*[19] introduced the threshold photon flows for Q-switched and continuous wave (CW) singly resonant IOPOs respectively, there was no experimental support. Wan *et al.*[20] and Qu *et al.*[21] qualitatively analyzed the effects of some parameters on the threshold of IOPO by use of the threshold expressions of EOPO. It was experimentally shown previously that the threshold pump densities of IOPOs were lower than those calculated by the threshold formulas of EOPO[22,23]. Therefore, to date there has been no detailed study on theory and experiment of the threshold pump intensity for a singly resonant IOPO at the same time.

In this paper, we derive the threshold pump intensity for a singly resonant IOPO based on the temporal theoretical model in Ref. [18]. Particular attention is paid to the dependence of the intracavity SRO threshold intensity on the signal wave output coupling. Meanwhile, a Nd:YAG laser pumped $KTiOPO_4$ (KTP) IOPO for eye-safe laser output is studied experimentally. In the experiment, we use four output mirrors with 60%, 70%, 80%, and 90% reflectivity at the signal wavelength. The measured threshold values are in good agreement with the theoretical data. With an output coupler reflectivity of 80%, a peak power of 70 kW at 1572 nm has been obtained at a repetition rate of 3.5 kHz. The pulse width is 4.9 ns. The investigation provides some theoretical and experimental guidance for optimum operation of IOPO.

Considering the mean-field approximation, we assume that the three waves are transversally single mode and single frequency. Moreover, we consider the pump field and signal field both experience the high-finesse cavities.

1671-7694/2008/030207-04

The electric fields for the three waves are

$$E_{\mathrm{p,s}}(z,t) = 2E_{\mathrm{p,s}}(t)\exp(ik_{\mathrm{p,s}}z)\exp[-i(\omega_{\mathrm{p,s}}t+\phi_{\mathrm{p,s}})] \times \exp[-(r^2/w_{\mathrm{p,s}}^2)], \quad (1)$$

$$E_{\mathrm{i}}^{\pm}(z,t) = 2E_{\mathrm{i}}^{\pm}(z,t)\exp(\pm ik_{\mathrm{i}}z)\exp[-i(\omega_{\mathrm{i}}t+\phi_{\mathrm{i}}^{\pm})] \times \exp[-(r^2/w_{\mathrm{i}}^2)], \quad (2)$$

where $E_{\mathrm{p,s}}(t)$ represent the pump and the signal amplitudes, respectively. $E_{\mathrm{i}}^{\pm}(z,t)$ represent the idler-field amplitudes in the two directions of propagation. $k_j = n_j\omega_j/c$ ($j = \mathrm{p,s,i}$) are the wave vectors for the pump, the signal, and the idler fields respectively, where ω_j are the frequencies, n_j are the effective refractive indices of the media, averaged over the cavity to avoid boundary problems. ϕ_j ($j = \mathrm{p,s,i}$) are the phases of the fields for each direction. w_j ($j = \mathrm{p,s,i}$) are the transverse waist radii of the three waves in the nonlinear crystal.

The nonlinear polarizations, generated by the three fields interacting in the nonlinear medium, are given by

$$P_{\mathrm{p}}^{\mathrm{NL}}(z,t) = \varepsilon_0\chi^{\mathrm{NL}}E_{\mathrm{s}}(z,t)\,E_{\mathrm{i}}(z,t),$$
$$P_{\mathrm{s}}^{\mathrm{NL}}(z,t) = \varepsilon_0\chi^{\mathrm{NL}}E_{\mathrm{p}}(z,t)\,E_{\mathrm{i}}^{*}(z,t),$$
$$P_{\mathrm{i}}^{\mathrm{NL}}(z,t) = \varepsilon_0\chi^{\mathrm{NL}}E_{\mathrm{p}}(z,t)\,E_{\mathrm{s}}^{*}(z,t), \quad (3)$$

where χ^{NL} is the nonlinear susceptibility of the medium, which is equal to the effective nonlinear coefficient d_{eff} in OPO.

The temporal evolution equations of the fields are described by[18]

$$\frac{\mathrm{d}A_{\mathrm{p}}}{\mathrm{d}t} + \frac{1}{\tau_{\mathrm{p}}}A_{\mathrm{p}} = -\frac{\omega_{\mathrm{p}}}{\varepsilon_0 n_{\mathrm{p}}^2}\mathrm{Im}(P_{\mathrm{p}}) - \frac{\omega_{\mathrm{p}}}{2\varepsilon_0 n_{\mathrm{p}}^2}\mathrm{Im}(P_{\mathrm{laser}}), \quad (4)$$

$$\frac{\mathrm{d}A_{\mathrm{s}}}{\mathrm{d}t} + \frac{1}{\tau_{\mathrm{s}}}A_{\mathrm{s}} = -\frac{\omega_{\mathrm{s}}}{\varepsilon_0 n_{\mathrm{s}}^2}\mathrm{Im}(P_{\mathrm{s}}), \quad (5)$$

$$\frac{n_{\mathrm{i}}}{c}\frac{\partial A_{\mathrm{i}}^{\pm}}{\partial t} \pm \frac{\partial A_{\mathrm{i}}^{\pm}}{\partial z} + \alpha_{\mathrm{i}}A_{\mathrm{i}}^{\pm} = -\frac{\omega_{\mathrm{i}}}{2\varepsilon_0 n_{\mathrm{i}}c}\mathrm{Im}(P_{\mathrm{i}}^{\pm}), \quad (6)$$

where α_{i} is the linear absorption of the nonlinear crystal at the idler frequency. τ_{p}, τ_{s} are cavity lifetimes for the pump and the signal fields respectively, which are as follows:

$$\tau_{\mathrm{p,s}} = \frac{2n_{\mathrm{p,s}}L_{\mathrm{laser,OPO}}}{c}\frac{1}{(1-R_{\mathrm{p,s}})}, \quad (7)$$

where $R_{\mathrm{p,s}}$ are reflectivities of the output mirror of the pump laser and signal laser respectively. L_{laser}, L_{OPO} are geometrical lengths of the laser cavity and the OPO cavity respectively. $\mathrm{Im}(P_{\mathrm{laser}})$ is the imaginary part of the projection of the laser-medium polarization on the laser-field spatial mode. $\mathrm{Im}(P_j)$ ($j = \mathrm{p,s,i}$) are expressed as[18,19]

$$\mathrm{Im}(P_{\mathrm{i}}^{\pm}) = -\varepsilon_0 d_{\mathrm{eff}}A_{\mathrm{p}}A_{\mathrm{s}}\sin(\Delta\phi^{\pm}), \quad (8)$$

$$\mathrm{Im}(P_{\mathrm{p}}) = \varepsilon_0 d_{\mathrm{eff}}^2\frac{2}{(1+(w_{\mathrm{p}}^2/\bar{w}_{\mathrm{p}}^2))}\left(\frac{l_{\mathrm{opo}}}{L_{\mathrm{laser}}}\right)A_{\mathrm{s}}^2A_{\mathrm{p}} \times \frac{\omega_{\mathrm{i}}}{2cn_{\mathrm{i}}}\frac{l_{\mathrm{opo}}}{2}\left(1-\frac{\alpha_{\mathrm{i}}l_{\mathrm{opo}}}{3}\right)\sin^2(\Delta\phi), \quad (9)$$

$$\mathrm{Im}(P_{\mathrm{s}}) = -\varepsilon_0 d_{\mathrm{eff}}^2\frac{2}{(1+(w_{\mathrm{s}}^2/\bar{w}_{\mathrm{s}}^2))}\left(\frac{l_{\mathrm{opo}}}{L_{\mathrm{opo}}}\right)A_{\mathrm{p}}^2A_{\mathrm{s}} \times \frac{\omega_{\mathrm{i}}}{2cn_{\mathrm{i}}}\frac{l_{\mathrm{opo}}}{2}\left(1-\frac{\alpha_{\mathrm{i}}l_{\mathrm{opo}}}{3}\right)\sin^2(\Delta\phi), \quad (10)$$

where $\bar{w}_{\mathrm{s,p}}$ are the waist radii of the nonlinear polarization, which are related to the field waists by $1/\bar{w}_{\mathrm{s,p}}^2 = 1/w_{\mathrm{s,p}}^2 + 1/w_{\mathrm{i}}^2$, moreover, $1/\bar{w}_{\mathrm{i}}^2 = 1/w_{\mathrm{i}}^2 = 1/w_{\mathrm{s}}^2 + 1/w_{\mathrm{p}}^2$. l_{opo} is geometrical length of the nonlinear crystal. $\Delta\phi = \phi_{\mathrm{p}} - \phi_{\mathrm{i}} - \phi_{\mathrm{s}}$.

It is evident from Eq. (5) that the threshold of IOPO is determined by setting $\mathrm{d}A_{\mathrm{s}}/\mathrm{d}t = 0$ since the terms on the right-hand side of the equation must exceed the decay terms $A_{\mathrm{s}}/\tau_{\mathrm{s}}$ for $\mathrm{d}A_{\mathrm{s}}/\mathrm{d}t$ to be positive. We set $\Delta\phi = \pi/2$ in order to maximize the nonlinear coupling. Substituting Eqs. (7) and (10) into Eq. (5), and using the relation $I_0 = \frac{1}{2}nc\varepsilon_0E_{\mathrm{p}}^2$, the threshold pump intensity for a singly resonant IOPO is given by

$$I_{\mathrm{pth}} = \frac{n_{\mathrm{p}}n_{\mathrm{s}}n_{\mathrm{i}}c^3\varepsilon_0(1-R_{\mathrm{s}})\left(1+\frac{\alpha_{\mathrm{i}}l_{\mathrm{opo}}}{3}\right)}{2\omega_{\mathrm{s}}\omega_{\mathrm{i}}d_{\mathrm{eff}}^2l_{\mathrm{opo}}^2}\left(\frac{w_{\mathrm{s}}^2+w_{\mathrm{p}}^2}{w_{\mathrm{p}}^2}\right) = \frac{n_{\mathrm{p}}n_{\mathrm{s}}n_{\mathrm{i}}c^3\varepsilon_0(1-R_{\mathrm{s}})\left(1+\frac{\alpha_{\mathrm{i}}l_{\mathrm{opo}}}{3}\right)}{2\omega_{\mathrm{s}}\omega_{\mathrm{i}}d_{\mathrm{eff}}^2l_{\mathrm{opo}}^2g_{\mathrm{s}}}, \quad (11)$$

where $g_{\mathrm{s}} = \frac{1}{1+(w_{\mathrm{s}}/w_{\mathrm{p}})^2}$ is the spatial overlap factor. It is seen that the intracavity SRO threshold intensity is dependent on the crystal length, crystal quality, signal wave output coupling, and pump and signal spot sizes.

Figure 1 shows the experimental setup for our IOPO. The pump module consisted of 12 diode bars (808-nm wavelength, 20-W output power). The water faucet of the pump module can be connected to a water-cooled temperature control system. The Nd:YAG rod (3 mm in diameter, 75 mm in length) was plane-parallel polished and anti-reflection coated on both ends at 1.064 μm. The overall Nd:YAG laser cavity was formed by two high reflecting mirrors: $\mathrm{M_1}$ and $\mathrm{M_2}$. The rear mirror $\mathrm{M_1}$ was a 2-m radius of curvature concave mirror with

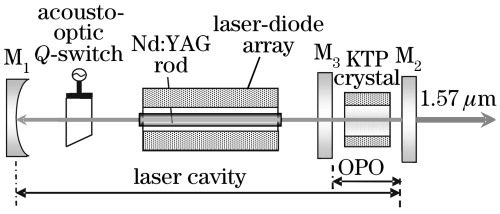

Fig. 1. Schematic diagram of the IOPO.

high reflectivity at 1.064 μm, whereas the M_2 mirror was highly reflective at 1.064 μm and partly reflection (R_s) at the signal parametric wavelength of 1.57 μm. The OPO cavity, 30 mm long, was formed by a pair of plane-parallel mirrors: M_2 and M_3. M_3 was anti-reflective at 1.064 μm and highly reflective at $1.55 - 1.63$ μm. The uncoated KTP crystal of the size $5 \times 5 \times 18.8$ (mm) was x-cut for the type II noncritical phase matching ($\theta = 90°$, $\phi = 0°$) in order to maximize the effective nonlinear coefficient and essentially eliminate walk-off between the pump, signal, and idler beams. Moreover, it was mounted in a water-cooled copper block with indium foil wrapped to improve the thermal conduction between the crystal and the copper heat sink. The temperature of the copper mount was kept at 16 °C during the operation of the laser. Because of the low reflectivity of the OPO mirrors at idler wavelength, the singly resonant IOPO scheme is accomplished.

Figure 2 shows the threshold pump intensity as the function of the output reflectivity at signal wavelength. The parameters used in the calculation are as follows: $c = 3 \times 10^8$ m/s, $n_p = 1.748$, $n_s = 1.737$, $n_i = 1.771$, $d_{eff} = 3.64$ pm/V, $\varepsilon_0 = 8.854$ pF/m, $\alpha_i = 0$, $g_s = 0.8$[22]. From Fig. 2, it can be seen that the theoretical threshold decreases as the output reflectivity increasing. In the experiment of IOPO, we used four output coupler reflectivities of 60%, 70%, 80%, and 90% at 1572 nm. The experimental threshold values were derived by measuring the leaking pump pulse power and width before the onset of the parametric oscillation. The results show that experimental results are in excellent agreement with the theoretical threshold analysis for the IOPO. The threshold of IOPO is several MW/cm^2, which is much lower than that of EOPO. We also calculated the threshold based on the equation for EOPO in Ref. [15], plotted in the same figure. The data is higher than the experimental value.

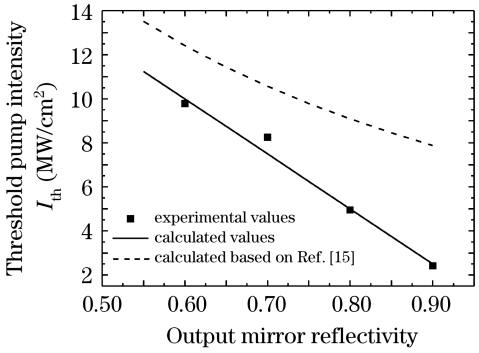

Fig. 2. Oscillation threshold of the KTP-IOPO versus output mirror reflectivity.

When three output coupler reflectivities of 60%, 70%, and 80% were employed, the average output power at 1572 nm was measured at a repetition rate of 3.5 kHz, as shown in Fig. 3. It is seen that the OPO laser has the lowest threshold when the output reflectivity is 80%. In this case, the theoretically calculated threshold is 4.9558 MW/cm^2, whereas the experimentally measured value is 4.9972 MW/cm^2. Average power of 1.2 W for the signal wave was achieved when the pump current was 20 A. Without KTP-OPO cavity, the pump power of 1064 nm was 9.3 W with 10% transmittance at 1064 nm. Therefore, the conversion efficiency from Q-switched output at 1064-nm wavelength to OPO signal output power is 12.9%. In Fig. 3, we also find that the OPO output reaches to saturate and decreases eventually at higher pump currents. One possible reason is that optical absorption of the idle wave in KTP crystal will lead to the development of thermally induced lens in OPO crystal[24]. This will reduce the mode volume and decrease the output power. The other reason may be the degeneration of beam quality of the 1.064-μm laser which is induced by the increasing thermal effect in Nd:YAG crystal with the increase of diode pumping power.

For the IOPO we measured the average power of the signal output as a function of the repetition rate with an output reflectivity of 80%, as shown in Fig. 4. Basically, the threshold pump intensity of IOPO increases with the increase of repetition rate. This is because that the higher repetition rate will lead to a lower peak power of the pump laser. However, there exists an optimum value of the inverse population density at threshold. It corresponds to an optimum repetition rate. The maximum power of 1.2 W at 1572 nm was obtained at a repetition rate of 3.5 kHz in our experiment.

Figure 5 depicts the signal pulse width (full-width at half-maximum, FWHM) as a function of the pump current for different reflectivities of the output mirrors at a repetition rate of 3.5 kHz. At a certain current, the discrepancies of the pulse widths are not significant for different couplers because of the effective cavity dump of the IOPO. The temporal characteristics of pump and signal pulses at the pump current of 20 A, recorded with 80% reflectivity on the output coupler, are shown in Fig. 6. When the pump width of 1064 nm was about

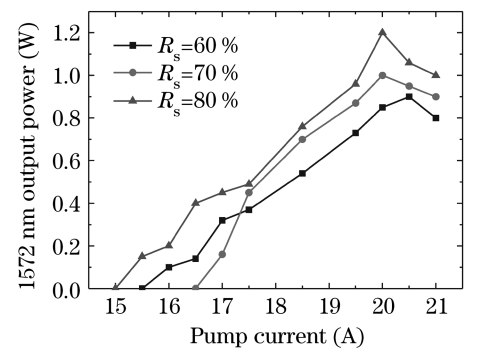

Fig. 3. Average output power at 1572 nm with different output mirrors versus pump current.

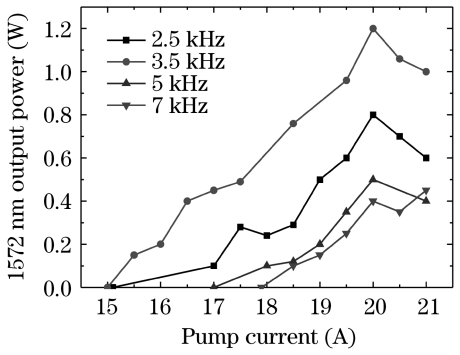

Fig. 4. Average output power at 1572 nm versus pump current for different repetition rates when $R_s = 80\%$.

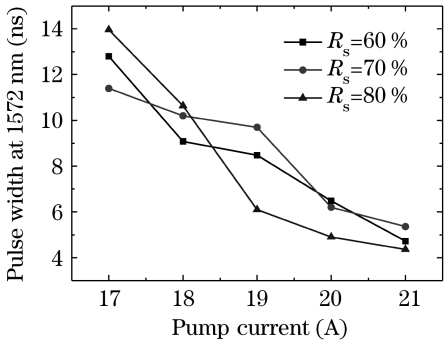

Fig. 5. Pulse width (FWHM) at 1572 nm with different output mirrors versus pump current.

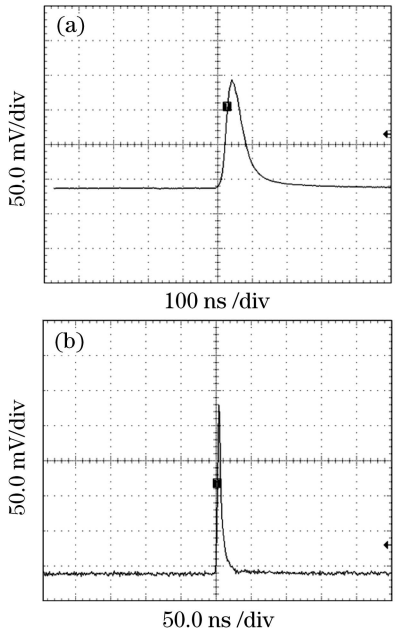

Fig. 6. Temporal profiles of the pump and signal pulses at 3.5 kHz under the pump current of 20 A when $R_s = 80\%$. (a) Pump pulse; (b) signal pulse.

53.8 ns, 4.9-ns duration pulse for 1572 nm was achieved. As a result, the peak power of signal wave amounted to 70 kW. Therefore, an effective high-peak-power high-repetition-rate 1.57-μm laser can be realized through optimization of the signal reflectivity of the output mirror and the pulse repetition rate.

In summary, the threshold pump intensity for a singly resonant IOPO has been derived from the temporal coupled field model. We analyzed the influence of the signal wave output coupling on the intracavity SRO threshold intensity. Meanwhile, a singly resonant pulsed KTP IOPO pumped by an acousto-optic (AO) Q-switched Nd:YAG laser was studied experimentally. The experiment was performed with four signal wave output reflectivities of 60%, 70%, 80%, and 90%. The measured threshold values are in good agreement with the theoretical data. When the output reflectivity is 80%, up to 70 kW peak power with 4.9-ns duration at 1572 nm for 3.5-kHz repetition rate was demonstrated. The investigation can provide some theoretical and experimental guidance for optimum operation of IOPO.

This work was supported by the National Natural Science Foundation of China (No. 10474071) and the Ph.D. Programs Foundation of Ministry of Education of China (No. 20040056010). Y. Wang's e-mail address is wangyuye2000@163.com.

References

1. M. K. Oshman and S. E. Harris, IEEE J. Quantum Electron. **4,** 491 (1968).
2. E. O. Amman, J. M. Yarborough, M. K. Oshman, and P. C. Montgomery, Appl. Phys. Lett. **16,** 309 (1970).
3. R. S. Conroy, C. F. Rae, G. J. Friel, M. H. Dunn, and B. D. Sinclair, Opt. Lett. **23,** 1348 (1998).
4. R. F. Wu, K. S. Lai, H. F. Wong, W. J. Xie, Y. L. Lim, and E. Lau, Opt. Express **8,** 694 (2001).
5. Y. F. Chen, S. W. Chen, S. W. Tsai, and Y. P. Lan, Appl. Phys. B **76,** 263 (2003).
6. W. Zendzian, J. K. Jabczynski, P. Wachulak, and J. Kiatkowski, Appl. Phys. B **80,** 329 (2005).
7. Y. Wang, D. Xu, Y. Yu, W. Wen, J. Xiong, P. Wang, and J. Yao, Chin. Opt. Lett. **5,** 93 (2007).
8. J. E. Bjorkholm, IEEE J. Quantum Electron. **5,** 293 (1969).
9. J. E. Bjorkholm, IEEE J. Quantum Electron. **7,** 109 (1971).
10. S. J. Brosnan and R. L. Byer, IEEE J. Quantum Electron. **15,** 415 (1979).
11. S. Guha, F.-J. Wu, and J. Falk, IEEE J. Quantum Electron. **18,** 907 (1982).
12. J. A. C. Terry, Y. Cui, Y. Yang, W. Sibbett, and M. H. Dunn, J. Opt. Soc. Am. B **11,** 758 (1994).
13. D.-H. Lee, M. E. Klein, and K.-J. Boller, Appl. Phys. B **66,** 747 (1998).
14. S. Schiller, K. Schneider, and J. Mlynek, J. Opt. Soc. Am. B **16,** 1512 (1999).
15. L. R. Marshall and A. Kaz, J. Opt. Soc. Am. B **10,** 1730 (1993).
16. W. Koechner, *Solid-State Laser Engineering* (in Chinese) W. Sun, Z. Jiang, and G. Cheng (trans.) (Science Press, Beijing, 2002) p.540.
17. L. Neagu, C. Ungureanu, R. Dabu, A. Stratan, C. Fenic, and L. Rusen, Opt. Laser Technol. **39,** 973 (2007).
18. T. Debuisschert, J. Raffy, J.-P. Pocholle, and M. Papuchon, J. Opt. Soc. Am. B **13,** 1569 (1996).
19. G. A. Turnbull, M. H. Dunn, and M. Ebrahimzadeh, Appl. Phys. B **66,** 701 (1998).
20. Y. Wan, Q. Y. Zeng, D. Y. Zhu, K. Han, T. Li, H. Han, S. F. Yu, and X. Z. Su, Chin. Phys. **13,** 1402 (2004).
21. Y. Qu, Y. F. Li, Y. M. Sun, X. Y. Hou, and H. J. Qi, Opt. Laser Technol. **39,** 715 (2007).
22. A. Agnesi, S. Dell'Acqua, and G. Reali, Appl. Phys. B **70,** 751 (2000).
23. J. G. Miao, H. M. Tan, H. K. Bian, B. S. Wang, and J. Y. Peng, Opt. Commun. **265,** 349 (2006).
24. M. S. Webb, P. F. Moulton, J. J. Kasinski, R. L. Burnham, G. Loiacono, and R. Stolzenberger, Opt. Lett. **23,** 1161 (1998).